

# Advances in Wave Resource Estimation: Measurements and Data Processing

J Cruz<sup>1</sup>, E Mackay<sup>2</sup> and T Martins<sup>1</sup>

<sup>1</sup> Ocean Power Delivery Ltd, 104 Commercial Street  
EH6 6NF, Edinburgh, UK  
j.cruz@oceanpd.com

<sup>2</sup> National Oceanography Centre, University of Southampton  
European Way, SO14 3ZH, Southampton, UK  
eblm@noc.soton.ac.uk

## Abstract

New software has been developed by Ocean Power Delivery to process data from directional Waverider buoys. The software improves on existing packages by providing robust quality checking of the input time series, user definable options for spectral analysis and several advanced methods of directional analysis. Significant differences in parameters important to Wave Energy Converter (WEC) performance were noted when compared to the conventional processing. If not addressed, these differences can lead to inaccuracies when calculating WEC performance.

The use of satellite altimeter data for long term resource prediction is also discussed. A new algorithm for estimating the wave period from altimeter data has been developed jointly by Ocean Power Delivery and the National Oceanography Centre, Southampton (NOC). The algorithm is a significant improvement on previous models which were unable to properly reproduce the joint distribution of wave height and period, a necessity when estimating device response. The new algorithm enables mean monthly and annual Pelamis power output to be calculated to a high accuracy at any location in the world.

**Keywords:** Wave Energy Resource Assessment, Buoy Measurements, Satellite Altimeter Wave Measurements, Pelamis WEC.

## Nomenclature

$S(f)$	frequency spectrum
$S(f, \theta)$	directional spectrum
$m_n = \int f^n S(f) df$	spectral moment ( $n^{\text{th}}$ order)
$H_{m0} = 4\sqrt{m_0}$	significant wave height
$T_{-10} = m_{-1} / m_0$	energy period
$T_{01} = m_0 / m_1$	mean period
$T_{02} = \sqrt{m_0 / m_2}$	zero up-crossing period

## Introduction

The Pelamis wave energy converter continues to be developed by Ocean Power Delivery Ltd (OPD). Along with the engineering innovations that are emerging from the ongoing numerical modelling and validation programme, significant improvements are being achieved in wave data monitoring and processing applications. A new set of computational packages are being developed, in analogy to what occurred with the wind energy industry.

The ability to accurately measure the waves at a given site is essential for the development of wave energy as a commercial prospect. The long term resource at potential sites must be assessed in advance of a project going ahead. The variability and uncertainty of the resource estimate must also be clearly understood. Equally essential is an accurate measurement and analysis of the waves incident on an installed WEC, so that its performance can be monitored and optimised.

To this end, two sets of tools have been developed. A first package contains several modules: a statistical toolbox, which is able to load data directly from a Pelamis machine, compile it statistically and fit standard mathematical distributions to it; a fatigue toolbox, which can be used to determine the life span of certain components; a report generator toolbox, which through a graphical user interface allows the creation of summaries of data and key derived variables, such as mechanical absorbed power, electrical power, capture width and efficiency; and finally a wave analysis toolbox, which imports data from wave measurement systems such as Waverider buoys and processes it, extending the conventional tools that are currently used. The latter is described in detail in this paper. The second package uses satellite altimeter data to predict the long term wave resource at any site in the world. This is described in the final section of this paper.

It should be emphasised that the studies described in the present paper are relevant for the current generations of Pelamis machines: the full-scale prototype and the Portuguese P1-A machines, and also the starting point for the next generations, particularly when addressing the

monitoring of a first large scale offshore wave farm. The tools described in the paper are either directly or indirectly applicable to alternative wave energy converters.

## Wave analysis toolbox overview

A package has been developed in MATLAB to process Pelamis and wave data. Datasets from either the full-scale prototype or the P1A Pelamis machines (Enersis Project in Portugal) can be analysed, and the outputs from each individual toolbox can be mutually loaded, increasing the flexibility of the analysis. A wave analysis package is among the newly created tools. The primary inputs are the original files from Datawell Waverider buoys. The possibility of analysing data from other wave measurement systems (e.g. ADCP) can easily be added in the source code.

The initial motivation was to develop an alternative that is better adjusted to the operational environment of a wave energy farm when compared to the existing post-processing tools. Datawell's package W@ves21 is used as a benchmark. Additional objectives were to provide a transparent methodology for the post-processing of the displacement signals from the buoys and to extend the functionalities of the software, particularly with regard to the estimation of the directional spectra. Prior to analysis, the input files (buoy displacement time series) are subject to a number of quality controls, detailed later in the paper.

A graphical user interface (GUI) was designed to assist the user in the processing tasks. The main GUI is divided into three main parts:

- Computation of omnidirectional frequency spectra and parameters (see figure 1)
- Computation of directional spectra with options to use different methods
- Display of data from multiple files, e.g. time series plots of spectral parameters, 3D histograms of wave height versus period (see figures 2-4).

For the omnidirectional spectral analysis, it is possible to define type of taper window and the length of the FFT. Details of directional spectra estimation are given in next section. The toolbox also allows the use of data of arbitrary lengths, i.e. the half hour input files can be joined together or split up to give parameters for a user-specified averaging period.

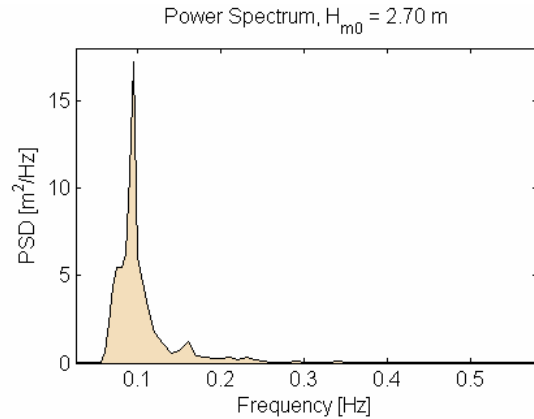


Figure 1: Power spectral density for a half hour record.

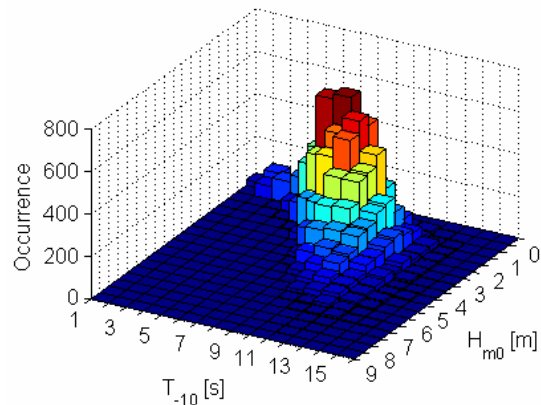


Figure 2: 3D histogram of  $H_{m0}$  and  $T_{10}$  for 1 year.

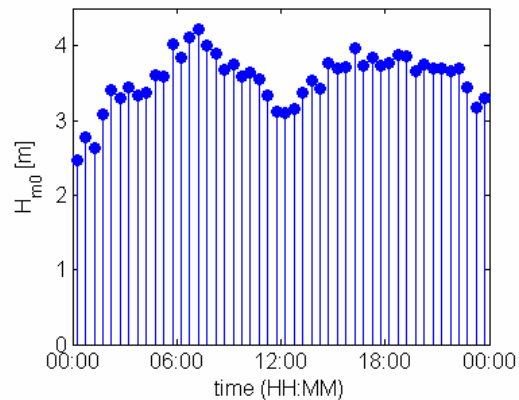
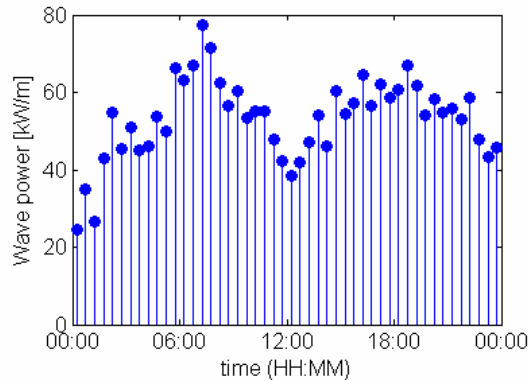


Figure 3: 30 min average  $H_{m0}$  for 1 day.



**Figure 4:** 30 min average wave power for 1 day.

## Directional spectrum estimation

The directional spectrum can be estimated using the displacements recorded in three independent directions: heave, surge and sway. OPD's package is a refinement of the DIWASP package, introduced in [1], including new transfer functions (which link buoy displacement to sea surface elevation, see [2]) and a custom made interface for single-point measurement systems. All the main stochastic and deterministic methods to obtain the directional spectrum were implemented, following [2]. In particular, it is possible to select between:

1. Stochastic Methods:
  - Truncated Fourier Series Decomposition Method (TFSM)
  - Direct Fourier Transform Method (DFTM)
  - Extended Maximum Likelihood Method (EMLM)
  - Iterated Maximum Likelihood Method (IMLM)
  - Extended Maximum Entropy Principle (EMEP)
  - Bayesian Directional Method (BDM)
2. Deterministic methods
  - Single Direction Decomposition (SDD)
  - Double Direction Decomposition (DDD)

The output can be plotted in a linear 3D frame or in polar coordinates (see figures 5-8).

To illustrate the influence of the estimation method in the calculation of the directional spectrum, the directional spectrum for a 30 minute record from a Waverider buoy is shown for four different methods (see figures 5-8). A wider discussion about the differences between a stochastic and a deterministic approach is justified in order to understand the full range of possibilities when estimating the directional spectrum.

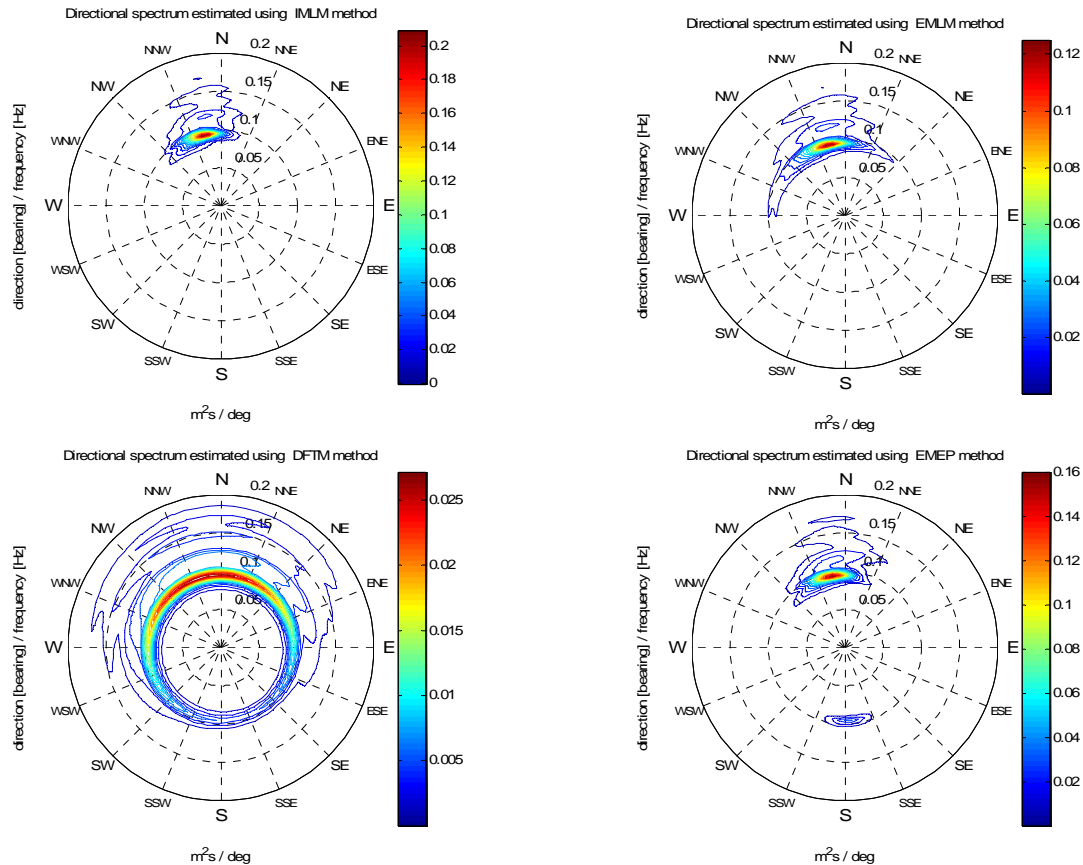
Stochastic methods are based on the random phase assumption. The cross-spectra between each pair of signals are calculated, and the directional spectrum is calculated by deriving the relation with the cross-spectra, using one of the available methods. The existence of a

directional spreading function, which if convoluted with the frequency spectrum results in the directional spectrum, is always assumed, but major differences exist when deriving it (i.e.: when fitting the data to the model): Fourier expansions use a deterministic fit, parametrical models use fixed form functions and the latest generation of methods, like the IMLM or EMEP, fit statistically to the data. The later class is by far the best option when modelling real data (particularly when evaluating data from Waverider buoys or any other single-point system).

Deterministic methods keep the phase information but only allow one or two directions per frequency. The cross-spectrum is not evaluated and the Fourier coefficients from each individual signal (surge, sway and heave) are used. The number of methods is much smaller than the stochastic equivalents and only two are typically used (SDD and DDD, single or double direction decomposition, respectively). The approach might prove particularly useful in cases where reflective structures are present.

For single-point measuring systems, such as a Waverider buoy, valid options are the EMLM, IMLM2, EMEP, SDD and DDD methods. A sensitivity study relating the major outputs ( $H_{m0}$ , dominant direction, etc.) and the analysis of the generated polar plots is helpful when quantifying the relative importance of the input options (like the frequency and directional resolutions, number of iterations, etc.). New methods continue to appear, such as the Wavelet directional method (see [4]), and it is likely that future versions of the toolbox will address even more methods.

Figures 5-8 show the estimated directional spectrum for selected methods, which differ considerably in terms of the degree of parameterisation and on the computational effort required, for the same frequency and directional resolution. It is therefore essential that the method is mentioned if estimates of the directional spectrum or of the directional spreading function are calculated. This is particularly important because the methods have different limitations and potentially erroneous conclusions can be extracted when looking at distributions if such information is not well established. As Figures 5-8 show, there are significant differences, and it seems clear that stochastic methods based on Fourier decompositions (e.g.: DFTM) are less suitable than those who fit statistically (e.g.: EMEP), as suggested in [2]. Datawell's approach tries to fit the original maximum entropy method derived in [3] to the Fourier approximation, but the results are presented in logarithm scale, which conceals most of the subtle variations. It seems more intuitive, clear and accurate to directly apply one of the last generation methods and present the output in linear scale. It is also clear that a single parameter like the mean wave direction is clearly insufficient to characterise the directionality of a given sea state (in the example presented in Figures 5-8 such parameter, when calculated using a energy conservation



**Figures 5 - 8:** Examples of the estimated directional spectrum using different methods (clockwise, from the top left: IMLM, EMLM, EMEP, DFTM).

approach, differs only five compass bearing degrees between all approaches, though there are substantial differences in the full directional spectrum).

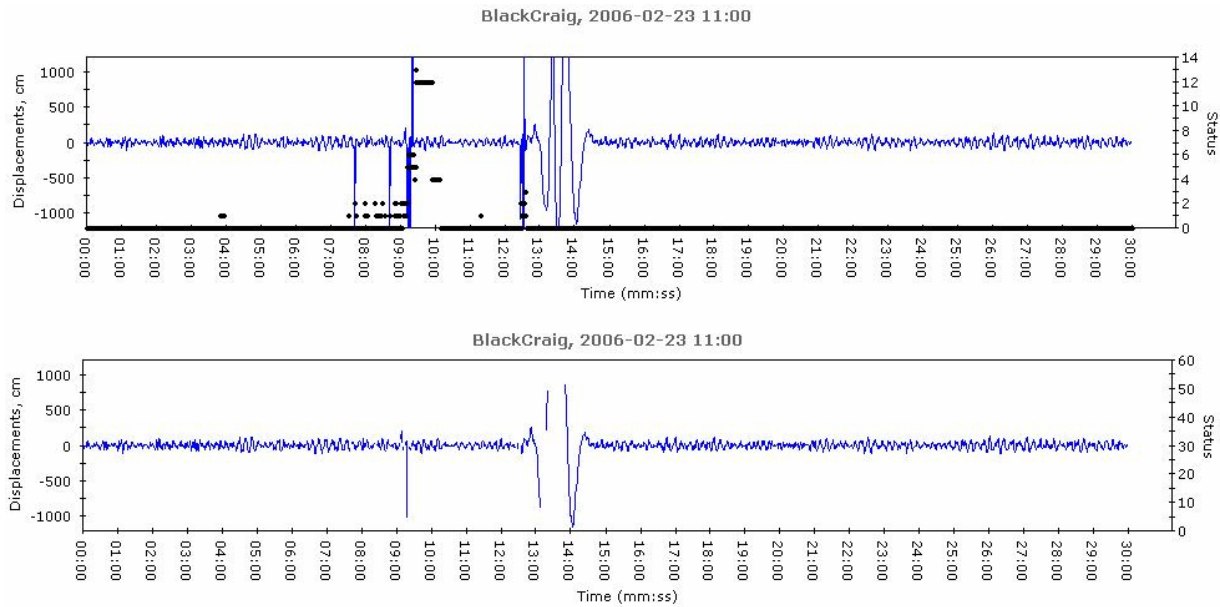
### Comparison between the MATLAB toolbox and W@ves21

In an effort to understand the differences between the two packages (MATLAB toolbox and W@ves21) it is relevant to provide more details about Datawell's approach. W@ves21 produces two frequency spectra for each displacement record. The spectra are tagged as 'buoy spectrum' and 'PC spectrum'. As the names suggest, the 'buoy spectrum' is computed on board the buoy, whereas the 'PC spectrum' is computed from the displacement signal transmitted to shore. The main difference in the two spectra is in the time periods they refer to. It should be noted that the 'buoy spectra' are not necessarily aligned to start on the hour or half hour, but start when the buoy is switched on. Moreover, the buoy's internal clock can drift with regard to GMT. 'PC spectra' are calculated using half hour records aligned to the start or end on the hour (according to the PC clock). The time offset between the 'PC' and 'buoy' spectra (somewhere between 30 and 60 minutes) can lead to differences in

wave power estimates as much as 30%. Therefore the parameters from the 'PC spectrum' were used for comparisons with those from the MATLAB toolbox.

It became clear that the handling of corrupted data needed to be addressed. When the displacement signal from the buoy is transmitted to land, errors in transmission can lead to spikes or extended periods of bad data. The receiving software checks the parity bits transmitted with the displacement signal to decide whether the transmission was completed successfully. Each data point is assigned a status flag according to the parity check. The flag is 0 if no errors are detected, 1 if an error was detected and repaired, and a value higher than 1 if the error could not be repaired. These records are saved as hexadecimal vectors with the extension \*.HXV. This system is generally robust. However, numerous cases of clearly bad data flagged with zero status have been observed.

When HXV files are open in W@ves21 there is an option to save the displacements as decimal vectors in files with the extension \*.RAW. These files are subject to other quality checks for which there is no documentation provided by Datawell. Figures 10-11



**Figures 10-11:** Example of a corrupted heave time series: using the HXV file (top) or using the RAW file (bottom).  
[Plot produced by W@ves21]

present an example of an HXV and corresponding RAW file, for where such errors were noticed. The value of  $H_{m0}$  is naturally influenced by these differences, being 10.63 m for the top figure and 2.32 m for the bottom one. From the figure it is also clear that even in the RAW file some bad data remains which will compromise the spectral parameters.

Finally it should be noted that another value of  $H_{m0}$  is displayed in the displacement tab of W@ves21, presumably calculated as 4 times the standard deviation of the heave signal (as opposed to a value related calculated from the spectrum), but again there is no documentation about how this value is calculated. By definition  $m_0$  is equal to the variance of the signal, but numerical inaccuracies from the FFT make it necessary to adjust the calculated spectrum so that  $m_0$  is equal to the variance (usually the adjustment is not more than a few percent). However, in W@ves21 the values of  $H_{m0}$  from the displacements and the spectra can differ considerably when there are errors in the data.

Datawell do not provide documentation on the quality controls and adjustments which lead to differences between parameters derived from displacements, HXV spectra and RAW spectra, nor do they state which values should be used in preference. This was a major driver for the development of the MATLAB toolbox, as the ability to control the quality of the data is of paramount importance to the wave energy community.

The MATLAB tools follow a transparent quality check procedure: firstly all samples with a transmission status above 1 (irreparable transmission error) are

removed. Then a spike detection test is conducted, following [5]. An excursion test is then applied, identifying individual waves for which a crest or trough exceeds  $5\sqrt{m_0}$ , as recommended by [6]. An initial estimate of  $H_{m0}$  is therefore necessary to apply such step. This is achieved by assuming that the surface elevation is normally distributed and using the inter-quartile range (IQR) to estimate the variance and hence  $m_0$ . The variance can be biased when there are outliers in the data, but the IQR will not be affected by these and is therefore a more robust estimator. The assumption of normality is valid when non-linear effects are insignificant (deep-water, low amplitude waves). Nonetheless, this approach for estimating  $H_{m0}$  proved accurate even in the largest seas where  $H_{m0}$  exceeded 10 m.

Figure 12 shows a comparison of the values of  $H_{m0}$  calculated from the IQR to the 'actual' value of  $H_{m0}$  calculated after quality control, for data from the EMEC site from January to March 2007. The plot shows excellent agreement: an orthogonal regression line fitted to the data has a slope of 0.997 and intercept of 0.005 m, with a residual RMS of 6 cm. Note that the data for this comparison was measured in a water depth of 50m and the method has not been tested for shallower locations where non-linear effects may be stronger.

If the steepness of a wave which fails the excursion check exceeds the breaking limit for deep-water waves ( $H/\lambda = 1/7$ ) then it is assumed to be bad data and is removed from the file, otherwise the file is flagged for further inspection. A final check ensures that the length of non-corrupted data analysed is greater than 15 min, or

alternatively that two blocks with 10 min of continuous non-corrupted data can be found. The calculation of the spectral parameters follows the four steps recommended in [7]: correction of the mean water level, application of a taper window before the Fourier analysis, computation of the Fourier coefficients and of the smoothed periodogram and a final adjustment of the energy, knowing that variance of the surface elevation must match  $m_0$ .

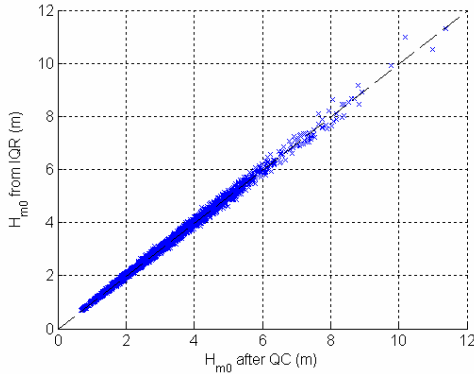


**Figure 12** Scatter plot of  $H_{m0}$  calculated from the IQR against  $H_{m0}$  calculated after quality control.

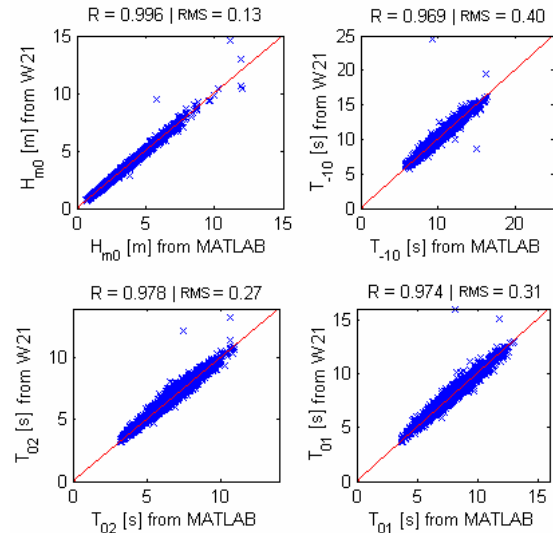


**Figure 13** Comparisons between W@ves21 and MATLAB parameters.

Figure 13 compares  $H_{m0}$ ,  $T_{-10}$ ,  $T_{02}$  and  $T_{01}$  calculated by W@ves21 (values from the ‘PC spectra’ from the HXV files) and the MATLAB toolbox. The analysis comprises 4316 records, spanning from January to March 2007 from the EMEC site. The correlation coefficient and the average RMS difference are presented for each parameter. All parameters generally show good agreement giving confidence to the MATLAB approach. Similar results were obtained for

other periods, so the procedure is not only transparent but robust.

The outliers in Figure 13 all occur because of differences between the quality checks which have been developed for the MATLAB toolbox and those used by W@ves21. Tables 1-2 summarise the values of  $H_{m0}$  and  $T_{02}$  for these outliers derived from the W@ves21 displacement tab, W@ves21 ‘PC spectrum’ from the HXV and RAW files, and from the MATLAB toolbox.

For the records 09/01 10:00 and 18/03 03:30, the HXV file has corrupted samples that were transmitted with status = 0, but the W@ves21 quality check procedures filter the data, leading to similar spectral parameters from the RAW file and the MATLAB approach. Figure 14 shows each step of the MATLAB quality check procedure for the ‘09/01 10:00’ case.

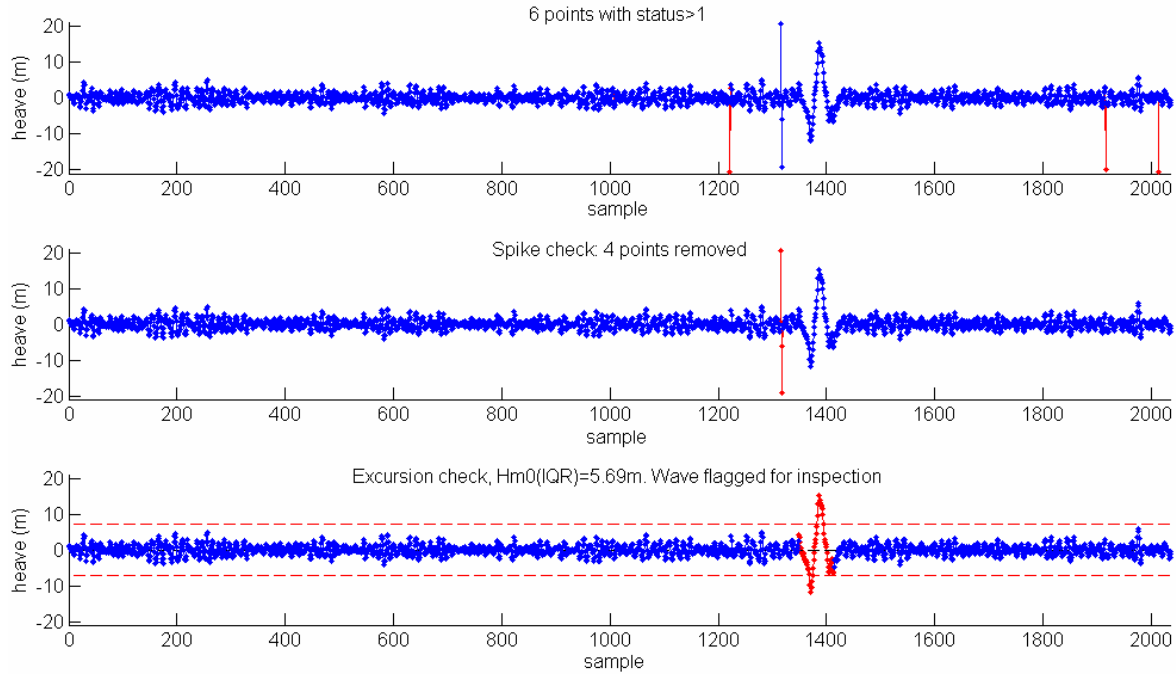
The ‘26/01 11:00’ case presents another relevant situation: although no errors are detected, the value of  $H_{m0}$  from the HXV ‘PC spectra’ differs considerably from the value given in the displacement tab. The number of samples in the record is shorter than expected, a not so uncommon situation in an operational scenario. It was subsequently proven that the value  $H_{m0}$  obtained via the HXV ‘PC spectrum’ is biased from shorter data files, and increasingly diverges from the RMS surface elevation as the time series becomes shorter.

For the records 18/03 04:00 to 18/03 05:00, the MATLAB minimum length criteria (15 minutes uninterrupted signal or two periods longer than 10 minutes) is violated and it would be discarded as it has insufficient good data. However, results are included here for comparison with W@ves21.

Finally, and as Table 2 suggests, with regard to  $T_{02}$  the values derived from the RAW files and from the MATLAB package are in close agreement, given that both are subject to quality check procedures. Figure 13 shows two outliers for this spectral parameter (09/01 10:00 and 18/03 03:30).

Date / Time	$H_{m0}$ (m)			
	HXV	RAW	Displ.	MATLAB
09/01 10:00	9.53	5.20	7.38	5.76
26/01 11:00	2.81	2.81	3.86	3.85
18/03 03:30	14.61	11.73	13.78	11.21
18/03 04:00	10.35	10.35	12.13	12.07
18/03 04:30	12.95	12.95	11.95	11.92
18/03 05:00	10.69	10.69	11.89	11.89

**Table 1** Comparisons between the values of  $H_{m0}$  for the outliers shown in Figure 13, calculated using different approaches.



**Figures 14:** MATLAB quality check procedures for HXV file from 09/01/2007 11:00

Date / Time	HXV	$T_{02}$ (s)	
		RAW	MATLAB
09/01 10:00	12.19	7.26	7.45
26/01 11:00	7.01	7.01	7.06
18/03 03:30	13.30	11.21	11.06
18/03 04:00	10.34	10.34	10.29
18/03 04:30	10.88	10.88	10.86
18/03 05:00	11.47	11.47	10.66

**Table 2** Comparisons between the values of  $T_{02}$  for the outliers shown in Figure 13, calculated using different approaches.

## Resource assessment using satellite altimeter data

It has been demonstrated by numerous authors that satellite altimeter data can be used to obtain accurate estimates of monthly and annual mean  $H_{m0}$  in offshore locations (e.g. [8], [9], [10]). The global coverage of satellite altimetry makes it a useful complement to measurements from buoys that, of necessity, are less extensively deployed. OPD and NOC have investigated the use of altimeter data to estimate the power produced by the Pelamis WEC in a large number of marine locations.

Altimeter measurements of significant wave height are widely accepted to be of comparable accuracy to that

of in-situ measurements (e.g. [11], [12]) Calculation of WEC power also requires knowledge of the wave period. A new algorithm to estimate wave period from Ku-band altimeter data has been developed jointly by OPD and NOCS, which enables  $T_{-10}$  and  $T_{02}$  to be estimated with RMS errors of around 1.0s and 0.6s respectively [13]. It is also shown that the algorithm is able to accurately reproduce the joint distribution of wave height and period. Comparisons between TOPEX measurements and NDBC buoy data are shown in Figure 15.

In [13] the new period algorithm (hereafter referred to as M07) is compared to the algorithms presented in [14] (hereafter G03) and [15] (hereafter Q04). Although less accurate than Q04, G03 is widely used so was included for completeness. The M07 algorithm reduces the RMS error in the measurement of  $T_{02}$  to 0.6s compared to G03 (RMS of 0.8s) and Q04 (RMS of 0.7s). It improves reproduction of the marginal distributions of period, significant steepness and the joint distribution of wave height and period; it has also reduced residual trends with wave height, period and steepness. In [13] it is shown that there is a limiting accuracy to a Ku-band altimeter wave period algorithm and that the M07 algorithm is very close to this.

Using altimeter measurements of wave height and estimates of period from the M07 algorithm it is possible to calculate the power generated by a WEC. OPD has constructed gridded  $2^\circ \times 2^\circ$  climatologies of mean monthly and annual Pelamis power using a global database of altimeter measurements from 6 missions, spanning 14 years [16]. An example for the North

Atlantic is shown in Figure 16. Note that the power scales have been omitted from these figures for commercial reasons.

In [16] a collocated dataset of altimeter and NDBC buoy measurements is used to assess the accuracies of monthly, annual and 10-year mean Pelamis power in a  $2^\circ \times 2^\circ$  square. The monthly and annual means were found to have rms errors of 34.3kW and 15.5kW respectively.

Maps of the wave climate in  $2^\circ \times 2^\circ$  squares are useful for locating areas of interest for wave energy development. However, implicit in this method is the assumption that wave conditions are the same over a  $2^\circ \times 2^\circ$  square. In coastal areas there is usually considerable spatial variability on this scale. Data along individual satellite passes can be analysed to give a finer resolution nearer shore, in areas of interest to wave farm developers. Even though measurements along individual tracks are sparse, with TOPEX/Poseidon and Jason on a 10 day repeat orbit, GFO 17 days, and ERS-2 and Envisat 35 days, there are many years of data for each satellite so that the long-term along-track averages are of a useful accuracy. An example using TOPEX, Poseidon and Jason data around the British Isles is shown in Figure 18. The along track resolution is sufficient to correlate with geographic and bathymetric features and are a useful extension to the wave climate maps.

The RMS errors of the mean Pelamis power along sections of the altimeter ground track are plotted against averaging time in Figure 19.

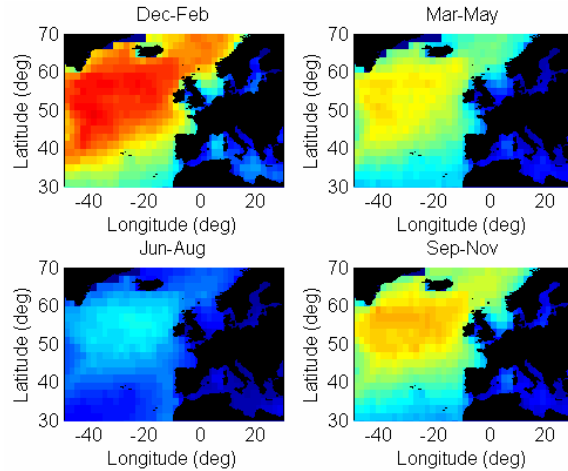


**Figure 16** Seasonal variation in Pelamis power over the North Atlantic from combined altimeter measurements.

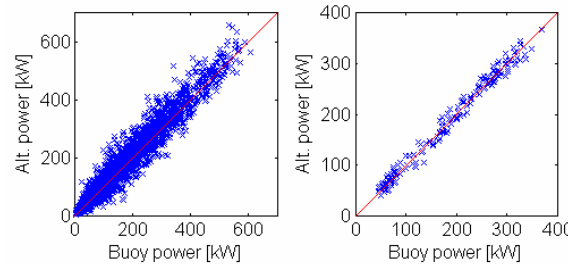


**Figure 17** Left: Scatter plot of monthly mean Pelamis power for buoy vs. altimeter measurements. Right: Scatter plot of annual mean Pelamis power for buoy vs. altimeter measurements.

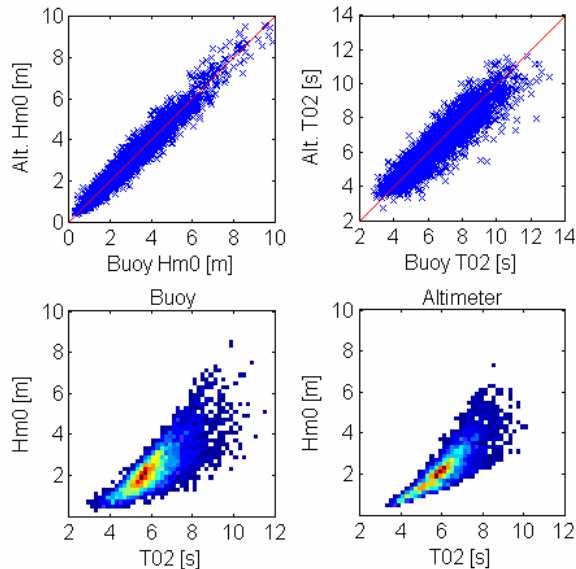


**Figure 15** Scatter plots of buoy vs. altimeter  $H_{m0}$  and  $T_{02z}$  (upper plots) and density plots of the joint distribution of  $H_{m0}$  and  $T_{02}$  (lower plots) from collocated TOPEX and NDBC buoy data.

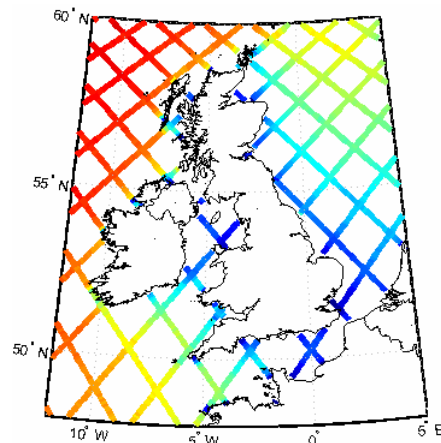


**Figure 18** Along-track mean Pelamis power for combined TOPEX/Poseidon and Jason phase A data for the period September 1992 – September 2006.

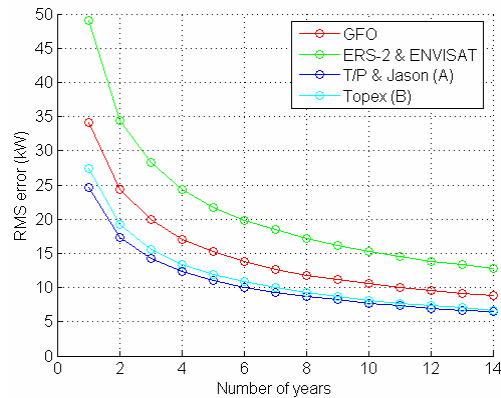


**Figure 19** RMS error in along-track Pelamis power against averaging period, for various sets of altimeter tracks [11].

## Conclusions

A new computational package to analyse data from Waverider buoys has been developed by Ocean Power Delivery. The major enhancements are linked with a fully controllable and transparent quality check procedure and with the capabilities of deriving the directional spectrum from a variety of methods. The methods have different limitations and potential, which must be kept in mind when interpreting the data. These two key features make the package more suitable for wave energy applications than other commercial packages. For OPD the link to the numerical simulation is already implemented, so real wave data can be used as input rather than simulated spectra. A validation exercise was conducted, using the spectral parameters obtained from W@ves21, Datawell's original post-processing package.

The MATLAB toolbox is likely to be extended to other measurement systems (e.g.: ADCP), and future work could include the use of the code to generate spectra in a wave tank. Further investigation is currently being conducted to better understand the physical reasons behind the corrupted data sets.

On the other end of the wave resource time scale, it has been demonstrated that it is possible to achieve an accurate estimate of the monthly and annual mean power produced by the Pelamis WEC in offshore locations by using altimeter data. Moreover, it has been shown that it is possible to gauge the spatial variability near to shore by using the along-track average values.

## Acknowledgements

Over the last few months there has been a useful dialogue with EMEC and Datawell. Eloi Droniou (EMEC) and Harry Noteborn (Datawell) are acknowledged for their efforts in the discussion.

## References

- [1] Johnson, D (2002). DIWASP, a directional wave spectra toolbox for MATLAB®: User Manual. Research Report WP-1601-DJ (V1.1), Centre for Water Research, University of Western Australia.
- [2] Benoit, M, Frigaard, P and Schäffer, HA (1997). Analysing Multidirectional Wave Spectra: A Tentative Classification of Available Methods, *Proc. IAHR Seminar on Multidirectional Waves and their Interaction with Structures, (27th IAHR Congress)*, San Francisco, USA, pp. 131-158.
- [3] Lygre, A and Krogstad, H (1986). Maximum Entropy Estimation of the Directional Distribution in Ocean Wave Spectra, *Journal of Physical Oceanography*, Vol. 16, pp. 2052-2060.
- [4] Donelan, M and Krogstad, H (2005). The Wavelet Directional Method. In: *Measuring and analysing the directional spectra of ocean waves*, EU Cost Action 714, pp. 71-80 (Ed. Khama et al.).
- [5] Longuet-Higgins MS (1985). Accelerations in steep gravity waves. *J. Physical Oceanography*, 15, 1570-1579.
- [6] Tucker MJ & Pitt EG (2001). *Waves in Ocean Eng. Elsevier Science Ltd, London*
- [7] Goda, Y (1985). *Random Seas and Design of Maritime Structures. University of Tokyo Press.*
- [8] Carter DJT, Foale S, Webb DJ (1991): Variations in global wave climate throughout the year. *International Journal of Remote Sensing*, Vol. 12, pp. 1687-1697
- [9] Young IR (1994): Global ocean wave statistics obtained from satellite observations. *Appl. Ocean Res.* 16,235-2
- [10] Woolf DK, Cotton PD, Challenor, PG (2002): Measurement of the offshore wave climate around the British Isles by Satellite Altimeter. *Philosophical Transactions of The Royal Society of London, Series A*, (2003), pp. 27-31
- [11] Krogstad HE & Barstow SF (1999): Satellite Wave Measurements for Coastal Engineering Applications. *Coastal Engineering*, 37, 283-307
- [12] Challenor PG & Cotton PD (2002): The joint calibration of altimeter and in situ wave heights. *World Meteorological Organization document number WMO/TD-No.1081*, JCOMM Technical Report No. 13
- [13] Mackay EBL, Retzler C, Challenor PG, Gommenginger CP (2007a): An Empirical Algorithm for Ocean Wave Period from Ku-band Altimeter Data. *In preparation (shortly to be submitted to Journal of Geophysical Research, Oceans).*
- [14] Gommenginger CP, Srokosz MA, Challenor PG (2003): Measuring ocean wave period with satellite

altimeters: A simple empirical model. *Geophysical Research Letters*, 30 (22).

[15] Quilfen Y, Chapron B, Serre M (2004): Calibration/Validation of an AltimeterWave Period Model and Application to TOPEX/Poseidon and Jason-1 Altimeters. *Marine Geodesy*, 27: 535–549.

[16] Mackay EBL, Retzler C, Challenor PG (2007b): Wave Energy Resource Estimation using the Satellite Altimeter. *In preparation (shortly to be submitted to Ocean Engineering)*.